Topics in In-situ Experiments with the HVEM at Osaka University

H. Mori

Research Center for Ultra-High Voltage Electron Microscopy, Osaka University, Yamadaoka, Suita, Osaka 565, Japan

(Received: Mar. 17, 1997 Accepted: Mar. 19, 1997)

Abstract

A few topics in in-situ experiments with the 3MV HVEM at Osaka University have been described. Issues included are (a) high temperature processes in refractory materials, (b) irradiation effects of MeV electrons, and (c) electromigration in Al lines for integrated circuits. It is shown that a variety of advantages of HVEM that cannot be afforded by conventional (100-200kV) and intermediate (300-400kV) voltage electron microscopy are effectively utilized in these studies.

1. Introduction

High voltage electron microscopy (HVEM) possesses a number of advantages that cannot be afforded by conventional electron microscopy. Examples are (i) the large observable thickness of specimens which is well above the critical thickness to reproduce the same phenomena as those occurring in bulk materials,(ii) simultaneous excitation of many reflections which is needed to observe microstructures in differently oriented grains at the same time,(iii) the high attainable spatial resolution due to the reduced wavelengh of electrons and (iv) the large space of the specimen chamber which makes it possible to incorporate a complicated, voluminous specimen-treatment device. Another unique advantage of HVEM is the fact that continuous observation of phenomena by a variety of electron microscopy techniques is possible simultaneously with the introduction of point defects.These unique benefits of HVEM have attracted special attention in recent years[1, 2].

In this contribution, a few topics of in-situ experiments with the 3MV HVEM at Osaka University will be presented.

2. In-Situ Experiments at High Temperatures

In-situ heating technique is one of the most important branches of in-situ HVEM experiments. The increasing demand for observations at very high temperatures in recent years has driven our research group to construct a hot stage capable of operation at temperatures of up to 2300K[3]. The heating system consists of a tantalum(Ta) tube specimen holder, surrounded by a coaxial Ta tube supporting a hearter filament of tungsten and two coaxial Ta thermal shields. The specimen, which is mounted at the tip of the holder, is heated by electron bombardment from the filament, and the temperature is controlled by adjusting the voltage (100-600V) applied between the filament and the specimen holder. With this stage set in the HVEM, a variety of high temperature processes have been studied in refractory materials. Two examples of such studies will be described below.

In the first example, the dissolution of hafnia particles into an alumina matrix at 2100K has been studied. It has been revealed that the dissolution of hafnia particles into the alumina matrix preferentially takes place via such lattice defects as grain boundaries. A similar preferential dissolution via grain boundaries has also been observed in the alumina-zirconia binary system . These observations demonstrate the important roles played by the lattice imperfections in determining the microstructures of the refractory materials at high temperatures.

In the second example, dislocation glide in sapphire at 1720K has been studied. In regions close to the tip of a crack, where the applied shear stress for the primary system is high, dislocations glide on the slip plane (basal plane) at a high velocity. In regions apart from the tip of a crack, where the applied shear stress for the primary system is low, dislocation motions are not necessarily confined to the slip plane and dislocations may undergo cross-slip or climb, depending upon the character of dislocations [4].

3. In Situ Irradiation Experiments

Using HVEMs, continuous observation of phenomena is possible simultaneously with the

introduction of point defects. Taking this advantage, our research group has carried out systematic studies to clarify the conditions under which non-equilibrium solid phases can successfully be produced under high-energy (MeV) electron irradiation.

3.1 Electron-Irradiation-Induced Amorphization

In 1982, it was discovered through HVEM studies that MeV electron irradiation can induce a crystalline-to-amorphous (C-A) transition in some intermetallic compounds such as NiTi and Fe_3B. The discovery of such an electron-irradiation-induced C-A transition is of considerable significance in view of the following points. The electron-irradiation-induced amorphization contains no quenching processes since the energy transferred to the primary knock-on atoms is sufficient to produce only single or at most double atom displacements. Thus through the discovery it becomes evident that production of cascade regions and quenching processes operating in the regions are not necessarily prerequisite for the C-A transition in crystals by particle irradiation, and that the amorphization by electron irradiation must be caused by a process in which the simplest types of crystal lattice defects play an essential role. It has been revealed that the C-A transition is a rather general phenomenon occurring not only in metallic compounds but also in non-metallic compounds and that the tendency toward the C-A transition is best correlated with the position of the compounds in the temperature-composition phase diagram. Namely, those compounds whose position in the phase diagram is close to the bottom of a deep valley of liquidus have a strong tendency toward the C-A transition, while those away from such a valley show little tendency toward the C-A transition. It has been suggested that the manifold in coordination, or in other words, the extent to which a variation is admissible in the atomic coordination in the material, is the most important parameter responsible for the amorphization tendency .

3.2 Electron-Irradiation-Induced Phase Decomposition in Intermetallic Compounds

It is generally accepted that an ordered alloy (or an intermetallic compound) either remains crystalline with a reduced degree of chemical order or undergoes a C-A transition when irradiated with MeV electrons at low temperatures where vacancies are thermally-immobile. Recently, however, it was found that besides these two modes of response there exists another mode of response where intermetallic compounds undergo a phase decomposition under low temperature irradiation [5]. For example it has been confirmed that Al3Ni decomposes into two phases under MeV electron irradiation; one is an aluminum-rich amorphous phase and the other crystallites of Al_3Ni_2.

A similar phase decomposition has been observed in such compounds as Al_2Cu and Al_4Pd. The finding of phase decomposition of this type is interesting in view of the following point; it is confirmed that the equilibrium to non-equilibrium phase transition which is induced by point-defect (and anti-site defect) introduction is not necessarily confined to single-phase to single-phase transitions such as an order-disorder transition and a C-A transition.

3.3 Electron-Irradiation-Induced Foreign-Atom Implantation

Hitherto foreign atom implantation into a solid has been carried out mainly by ion implantation. This ion implantation has now matured into an indispensable part of semiconductor technology. However in this method, the introduction of foreign atoms is limited to regions or positions right beneath the surface of the solid. Furthermore, severe irradiation damages are inevitably caused in the implantation regions.

A unique foreign-atom implantation technique in which irradiation effects of high energy (MeV) electrons are utilized has been put forward by H. Fujita [6]. The outline of the technique is as follows. First, a dopant phase comprising a target element is deposited either on the surface or the inside of the substrate. Here it is favorable that the target, dopant atom has a larger scattering cross-section for atom displacement than that of the solvent atom making up the substrate. For example, such a combination of an element with a high atomic number and a low melting point as a dopant and another element with a low atomic number and a high melting point as a substrate will be preferred. The composite specimen is then irradiated with electrons having an energy greater than the corresponding threshold energy

for atom displacement. Under irradiation the target atom in the dopant phase preferentially suffers elastic collisions with electrons and recoils with sufficient energy to intrude into the substrate. The repetition of the intrusion will result in the implantation of the target atom into the substrate.

Through a systematic study by the author's group, which has been carried out with the use of the HVEM, it has been revealed that this technique is applicable not only to systems with metallic substrates but also to those with nonmetallic substrates [7]. Applicability of the present technique to ceramic substrates has been investigated in the Au (target) / SiC (substrate), Pt/SiC , Hf/SiC , and Au/Si_3N_4 systems.

In the Au(target)/SiC(substrate) system, a new bonding state is formed between implanted-gold and silicon in the amorphous SiC substrate. Namely, injected gold atoms are chemically accepted in amorphous SiC. The formation of bonding between gold and silicon in amorphous SiC seems reasonable in view of the fact that the heat of formation for SiC and gold silicides are ca. 34 and 40KJ/mole, respectively. The repetition of the knocking-off and subsequent bonding result in the implantation of gold into the SiC substrate. Platinum atoms implanted into amorphous SiC bond with silicon. Hafnium atoms implanted into amorphous SiC bond with both silicon and carbon. On the other hand, gold cannot be implanted into Si_3N_4. The heat of formation for Si_3N_4 is ca. 100KJ/mole. This value is high compared to that for gold silicides(i.e., ca 40KJ/mole). Therefore, new stable bonding may be difficult to be formed between gold and silicon in Si_3N_4. It seems that such chemical constraint plays an essential role in determining the ease with which implantation into ceramics takes place [7].

4. Application to Issues in Advanced LSIs

A wide range of applications of the HVEM will involve material issues in advanced LSIs.

In situ observations of electromigration (EM) in Al lines for integrated circuits have employed various microscopy techniques, such as scanning electron microscopy (SEM) [8] and transmission electron microscopy (TEM) [see for example, Refs. [9-11] and references therein]. So far, TEM observations have been conducted solely in the plan-view mode, and such aspects as the preferential void evolution at the three-fold node of grain boundaries have been revealed [9]. However, in plan-view observations, it is difficult to get the vertically-resolved (in the depth direction) information on the microstructure in Al lines. Such depth-resolved information is indispensable for analyzing electromigration in the layered lines which are currently used in advanced LSIs, because the interlayer interfaces may play an essential role in these lines. Furthermore, in plan-view TEM samples, the Si substrate has to be locally thinned to a thickness of electron transparency. In such samples a non-uniform stress distribution due to both the local thinning and the local joule-heating along Al lines is often induced, which eventually leads to bending of the samples.

To overcome these drawbacks, we have developed a side-view TEM technique, in which an Al line on a thick substrate is observed with the HVEM with the incident beam parallel to the substrate surface and perpendicular to the Al line [12,13]. This technique utilizes the ability of HVEM to observe relatively thick samples. Additionally, since the substrate does not need to be thinned, difficulties encountered in the preparation and observation of conventional plan-view TEM samples can be avoided. With the use of this technique, successive stages of EM-induced void formation at the cathode and of EM-induced hillock formation at the anode in Al-on-TiN lines have been studied [14].

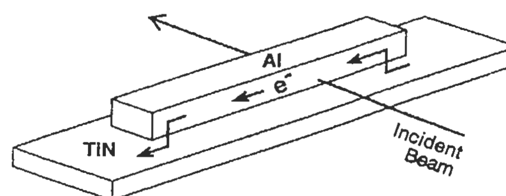

Fig. 1 Schematic illustration of side-view TEM observation employed in the present work. Arrows indicate electron flow.

An Al-on-Ti/TiN line with a drift-velocity-measurement structure, which provides information on electromigration in a line without reservoirs, was fabricated on an oxidized Si wafer (Fig.1). This structure consisted of an Al overlayer lying on the central part of a Ti/TiN underlayer conductor [9]. Both the Ti and TiN layers were 0.2μm thick. The length of the Ti/TiN portion between the bonding pad and the Al was 120μm. The Al

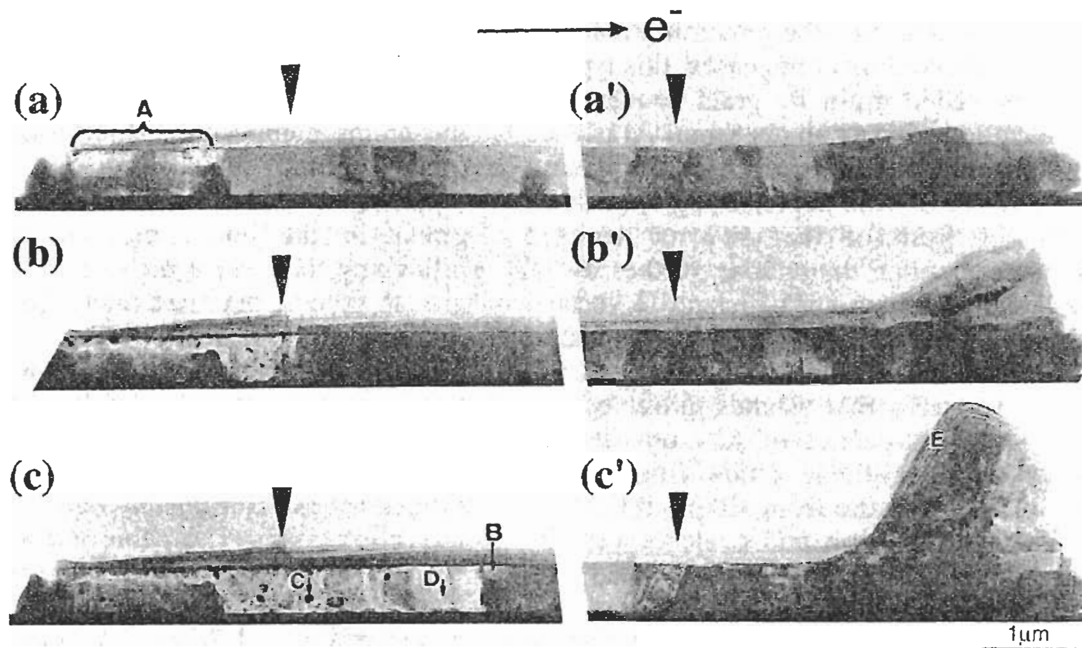

Fig. 2 Successive stages of electromigration in an Al-on-TiN line observed by side-view TEM. Damage evolution at the cathode and the anode of the line during current feeding are depicted in Figs. (a) to (c) and Figs. (a') to (c'), respectively. Current feeding time t for each figure is as follows. (a) t=720s, (b) t=2.8ks, (c) t=7.4ks, (a') t=1.6ks, (b') t=2.9ks, and (c') t=7.6ks.

was 0.7μm wide, 0.5μm thick, and 100μm long. The samples used in these experiments varied in width of Ti/TiN underlayer. Sample 1 had a pure Al line on top of a 2μm wide Ti/TiN underlayer and Sample 2 also had a pure Al line, but the Ti/TiN underlayer was 0.7μm wide.

The Al lines were not passivated, but a thin photoresist layer remained on the surface after ashing in an oxygen atmosphere. The fabricated wafers were annealed in nitrogen gas at 723K for 1.8ks. The Al line exhibited a near-bamboo structure. A chip, ~0.5mm by ~6mm in size and 0.45mm thickness, was then diced from the wafer and served as the side-view HVEM sample. Neither the Al lines nor the silicon substrates were thinned prior to observation.

The Al lines were directly observed from the side with the HVEM operating at an accelerating voltage of 2 MV. The sample was heated during observation by the joule-heating predominantly at the Ti/TiN portions without overlayer Al. The temperature of the Al was not measured, but a comparison of the drift velocities obtained by in situ HVEM experiments with those from standard accelerated measurements suggested that the average temperature of the Al may have been between 573~623K.

Figure 2 shows the results of the experiment using Sample 1. A current of 50mA (current density j=~13MA/cm^2) was first fed for ~14 seconds. This stressing time was limited by the melting of the solder which bonded the current-feeding wires to the electrodes of the HVEM sample holder. After the solder bonds were repaired, the in-situ observation was resumed at a current of ~26mA (j=~6.5MA/cm^2). (In the text and the caption referring to Fig. 2, the feeding times of a 26mA current are designated as t).

Figure 2(a) is a bright-field (BF) image of the cathode of an Al-on-TiN line after feeding of the 26mA current for 720s (i.e. t=720s). A locally depleted region (A) was formed adjacent to the cathode edge. The same area after feeding for 2.8ks (i.e., t=2.8ks) is presented in Fig. 2(b), where it is shown that the depleted region extended ~2.5μm towards the anode from the cathode edge. Figure 2(c) shows the same area at t=7.4ks. At this stage, the depleted region extended over ~4.4μm from the cathode edge.

Two points are noteworthy in Fig. 2(c): (1) One of the characteristic depletion modes verified by side-view TEM appears at B in front of the

large depleted region in the figure. Void growth proceeds towards the substrate within a single grain; the top surface of the remaining material at B is (111) faceted. In some cases, this type of voiding proceeded grain by grain sequentially from the cathode end [13]. (2) Small Al islands are formed on the inner surface of the natural oxide film covering the depleted region. Islands close to the front of the growing depleted region were smaller than those further away. For example, the diameter of island D, located near the front, was about 10nm, whereas that of island C, further from the front, was about 100 nm. This suggests that islands grow by the diffusion and coalescence of Al atoms left on the inner surface of the oxide film. Larger islands further from the front simply reflect the extra time for diffusion and coalescence. The presence of well-defined facets associated with voids in front of the large depleted region, such as a facet seen at B in Fig. 2(c), shows that Al does not melt there and that melting of Al is not a cause of the island formation.

Figure 2(a') is a BF image of the anode of the same line after feeding of the 26mA current for 1.6ks (t=1.6ks), where a small hillock is noticed to be formed at the anode. In Fig. 2(b'), which was taken from the same area at t=2.9ks, it is shown that the hillock grew to a height of approximately 0.9μm. As seen in this figure, some grains within this hillock exhibited brightness completely different from those of the grains composing the original line, while other grains showed diffraction contrast reminiscent of the epitaxy of the corresponding grains in the line. This fact suggests that hillocking took place not only via an epitaxial growth process but via a nucleation and growth process and differently oriented grains were formed on the top surface of the anode. The microstructure at the interface between the original bamboo grains and the hillock, which might shed light on the mechanism behind the hillocking, is unfortunately not well resolved in this micrograph. The same area after feeding current for 7.6ks is shown in Fig.2(c'). At this stage, the height of the hillock reached approximately 1.7μm. In one of grains composing the hillock, there appears a series of equal thickness fringes, as seen at E in Fig. 2(c'). From the intervals between the neighboring fringes, it is possible to get information on the three-dimensional shape of the hillock. In the present case, a hillock in the

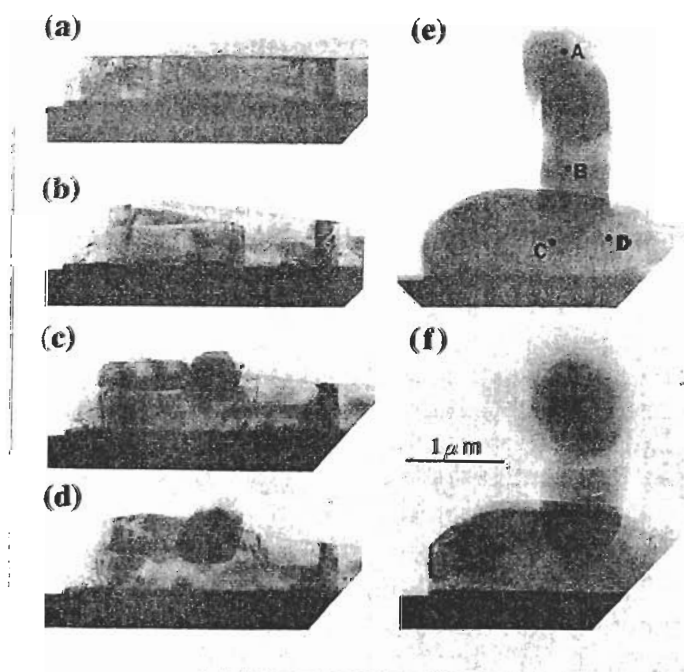

Fig. 3 Successive stages of whisker growth at the anode of an Al-on-TiN line. In this experiment, a 19mA current was first fed for 5.5ks and then the current was increased to 25mA. Current feeding time t is as follows. (a) t=0s, (b) t=4.08ks, (c) t=5.70ks, (d) t=6.18ks, (e) t=9.78ks, and (f) t=12.48ks. Electrons flowed from right to left. The width of the Ti/TiN layer in this sample was 0.7μm.

shape of a dome was deduced from such an analysis, and the shape was in agreement with the result by an independent SEM observation.
Figure 3 shows an example of whisker growth at the anode, which was observed in another pure Al sample (Sample 2). In this experiment, a 19mA current (j=~5MA/cm^2) was first fed for 5.5ks and then the current was increased to 25mA (j=~6.5MA/cm^2). Figure 3(a) is a BF image of the anode before current feeding. Figure 3(b) shows the same area after feeding 19 mA for 4.08 ks, where it is seen that a small hillock formed on the anode. The same area after feeding 19mA for 5.46ks and 25mA for 240s is shown in Fig. 3(c). At this stage, a small, faceted whisker appeared on the hillock. With continued current feeding, the whisker grew (Figs. 3(d) and (e)), and eventually the height of the whisker reached to approximately 1.6μm (Fig. 3(f)). Analysis of selected area electron diffraction (SAED) patterns taken from positions A to D of the whisker in Fig. 3(e) revealed that the whisker had a different orientation from the grain on which it nucleated and grew.
These side-view observations have provided information not obtainable by conventional plan-view TEM. It is revealed that frequently, voids were bounded by faceted Al planes and grew preferentially in the vertical direction in the grain in front of the large depleted region at the cathode. Polycrystalline hillocks grew partly in epitaxy to the grains in the line at the anode. A whisker, however, was found to have a crystallographic orientation different from the grains in the line.

5. Conclusion

In this paper, a few topics in in-situ experiments with the HVEM at Osaka University have been presented. It is evident that a variety of advantages of HVEM that cannot be afforded by conventional (100-200kV) and intermediate (300-400kV) voltage electron microscopy are effectively utilized in these studies. In the furure, by taking advantages of HVEM, in-depth studies will be made on individual subjects in materials science, especially in the development of advanced materials.

References

1. Ultramicroscopy 56, Nos. 1-3, (1994) eds. M. Rühle, F. Phillipp, A. Seeger and J. Heydenreich
2. Ultramicroscopy 39,Nos. 1-4, (1991) eds. H. Fujita, K. Ura and H. Mori
3. H. Mori, M. Komatsu and H. Fujita, Ultramicroscopy 51 (1993) 31
4. M. Komatsu, H. Mori, and K. Iwasaki, J. Am. Ceram. Soc., 77 (1994) 839
5. H. Mori and H. Fujita, Ultramicroscopy 39 (1991) 355
6. H. Fujita, In Situ Experiments with HVEM, ed. H. Fujita (ISBN 4-9900065-1-8), Osaka University (1985). P.1
7. H. Mori, T. Sakata, H. Yasuda and M. Maeda, J. Vac. Sci. Tech., B12 (1994) 2376
8. See for example, the following papers and references therein: R. W. Thomas and D.W.Calabrease, Proc. 1983 IEEE Int. Reliability Phys. Symp., p. 1; T. N. Marieb, E.
   Abratowski, J. Bravman, M. Madden and P. Flinn, in P. S. Ho, C-V. Li and P. Totta (eds.), Stress-Induced Phenomena in Metallization, AIP Conference Proc. 305, AIP, New York, 1994, p. 1.
9. L. Berenbaum, J. Appl. Phys. 42 (1971) 880.
10. A. Takaoka, N. Okaya, and K. Ura, Microsc. Microanal. Microstruct. 4(1993)239 .
11. C. Y. Chang and R. W. Vook, Thin Solid Films, 223 (1993)23 .
12. H. Okabayashi, H. Kitamura, M. Komatsu and H. Mori, Appl. Phys. Lett. 68 (1996)1066 .
13. H. Okabayashi, M. Komatsu and H. Mori, Jpn. J. Appl. Phys. Pt. 1, Vol. 35, No.2B (1996)1102.
14. H. Mori, H. Okabayashi and M. Komatsu, Thin Solid Films (1997) in press